Study of the wide-band viscous sound absorption behavior of lattices of rigid cylinders

Vicente Cutanda Henríquez[1], Martin A. Ibarias[2], José Sánchez-Dehesa[2]

[1] *Technical University of Denmark, Centre for Acoustic-Mechanical Micro Systems (CAMM), Ørsteds Plads, Building 352, 2800 Kgs. Lyngby, Denmark, E-Mail: vcuhe@dtu.dk*

[2] *Wave Phenomena Group, Department of Electronic Engineering, Universitat Politècnica de València, Camino de vera s/n (Building 7F), ES-46022 Valencia, Spain, E-Mail: maibaal1@upv.es, jsdehesa@upv.es*

Introduction

Viscous and thermal losses are an object of study since the establishment of acoustics as a branch of science [1,2]. More recently, acoustic losses have become an important issue in the design of both phononic crystals (PnCs) and acoustic metamaterials (AMTs) [3-9]. These improved designs include periodic corrugations or perforations [10], PnCs with gradient [11-12], and the use of optimization [13-15]. It has also been noted that viscous losses constitute in most cases 80% - 90% of the total viscothermal losses [6, 11, 16].

Different homogenization approaches exist that can obtain effective parameters (mass density, compressibility modulus and effective decay coefficient) of periodic distributions of rigid cylinders embedded in fluids [7,16,17,18]. By selecting and studying the effect of the homogenized parameters it is possible to understand and optimize their overall behavior.

In this work, we show how the selection of the lattice parameter a_0 and the viscosity of the medium affects the absorption of broadband sound in a PnC. We present both slab PnCs systems and finite PnC clusters of cylinders arranged in an isotropic hexagonal lattice. In both cases we demonstrate the existence of an optimal value of the filling fraction f for which a maximum wide-band absorption is obtained. This value varies in a range close to the maximum packing.

Theory

Decay coefficient in a phononic crystal

We describe the acoustic wave propagating in a homogenized 2D PnC as $p(x) = p_0 e^{\gamma_{ph} x} e^{i(kx-\omega t)}$, where γ_{ph} is the decay coefficient [7]. At the low frequency limit, it is shown to be

$$\gamma_{ph}(\hat{k}) = \frac{L_0}{2A_c c_{\text{eff}}(\hat{k})}\sqrt{\frac{\omega\eta}{2\rho}}\frac{M(\hat{k})}{N(\hat{k})} \qquad \text{m}^{-1} \qquad (1)$$

where $\hat{k}$ is the unit vector in the direction of propagation, L_0 is the circumference of the disperser, η the dynamic viscosity coefficient, ρ the density of the fluid, A_c is the area of the unit cell and $M(\hat{k})$ and $N(\hat{k})$ are functionals of the form factors in reciprocal space [7]. The effective speed of sound can be calculated as in [18, 19]. Eq. (1) is valid under some assumptions: the thickness of the viscous boundary layer $\delta = \sqrt{2\eta/\rho\omega} \ll \lambda$ and no overlapping of boundary layers. For a given frequency and value of the lattice parameter a_0, this condition determines the maximum filling fraction $f_{hex} = \frac{2\pi}{\sqrt{3}}\left(\frac{R}{a_0}\right)^2$, which, for a hexagonal network of rigid cylinders with radius R, is 0.9069. Additionally, the limit of maximum operating frequencies is determined by the first gap of firbidden frequencies [18].

Absorbance in a homogenized PnC slab

A homogenized PnC slab can be studied in one dimension, and the viscous absorbance can be deduced from the expressions of the transmission and reflection coefficients $r(\omega)$ and $t(\omega)$ as

$$R(\omega) = |r(\omega)|^2, \qquad (2)$$

$$T(\omega) = |t(\omega)|^2, \qquad (3)$$

$$\alpha(\omega) = 1 - R(\omega) - T(\omega). \qquad (4)$$

The coefficients $r(\omega)$ and $t(\omega)$ are given by the expressions in [19,20], which are functions of the frequency and γ_{ph}.

Quality factor Q

We define the absorption quality factor as

$$Q_\alpha^v = \frac{1}{\Delta\omega}\int_{\omega_b}^{\omega_t} \alpha(\omega) d\omega, \qquad (5)$$

where ω_b and ω_t are the lower and upper frequencies, and $\Delta\omega = \omega_t - \omega_b$ is the bandwidth. This parameter averages, in a single value, the absorption of the sample within a frequency band.

Model of an effective slab

A COMSOL model is prepared where losses are represented by the Boundary Layer Impedance (BLI) condition with only viscous, and no thermal, effects are activated [21]. The width of each layer of cylinders is $\sqrt{(3)}a_0/2$. The setup is shown in Figure 1.

With equations (4) and (5), it is possible to determine the amount of low-frequency absorption and characterize finite structures much faster and efficiently than using the Finite Element Method (FEM). The FEM (COMSOL) has, however, been employed to validate the analytical expressions.

Model of an effective cluster

We can homogenize circular clusters composed of N_c rigid cylinders into a single homogenized cylinder with an effective radius R_{eff} and effective acoustic parameters (c_{eff},

ρ_{eff} and γ_{eff}) [18]. The effective radius of the cluster is $R_{eff} = \left(N_c\sqrt{3}/2\pi\right)^{1/2}$ for a hexagonal lattice [22].

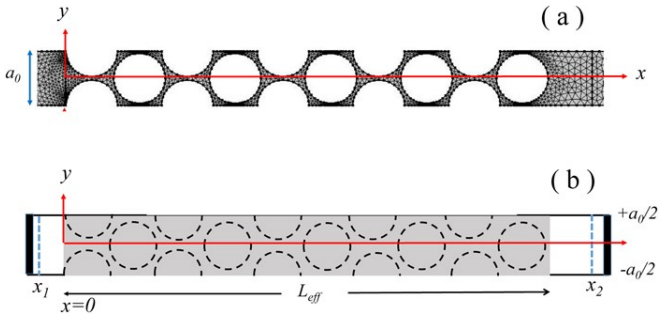

Figure 1: (a) COMSOL mesh of a PnC slab with 10 layers of rigid cylinders embedded in air. Floquet periodicity conditions are set on the y-axis and PML terminations on the sides. A plane wave arrives from the left. (b) The same structure after homogenization. The cylinders are distributed in a hexagonal network with a filling fraction of 0.8. $\boldsymbol{L_{eff}}$ is the effective length and $\boldsymbol{x_1}$ and $\boldsymbol{x_2}$ are the measurement positions.

The calculation of the reflectance, transmittance and absorbance is performed using the Boundary Element Method (BEM) with viscous losses [12,23,24]. Using a single fluid-like cylinder and the BEM, we can explore the influence of the filling fraction for circular clusters, as done on slabs.

Results and discussion

Results for PnC slabs

We define PnC slabs made with a fixed value of L_{eff} = 254 mm. We consider three lattice periods a_0= 7.5 mm, 11.6 mm and 15.46 mm which correspond to 30, 25 and 19 layers of cylinders respectively. The calculation considers three different background viscous media: air, glycerin and water. It is therefore necessary to use different frequency integration intervals, as shown in Table 1.

Table 1: Parameters in Fig. 2, limited by homogenization.

Viscous medium	$\omega_b/2\pi$ (Hz)	$\omega_t/2\pi$ (Hz)	$\Delta\omega/2\pi$ (Hz)	$\delta\sqrt{\omega}$ (m s$^{-1/2}$)
Air	580	3400	2820	8.872×10^{-5}
Water	2000	11500	9500	1.263×10^{-5}
Glycerin	4400	25800	21400	2.336×10^{-4}

We can observe a peak value of Q_α^v in Fig. 2 in all cases,. It can be explained in terms of the balance between the increase in viscous loss when the filling fraction increases and the decrease in the acoustic energy available for dissipation due to the increase in reflectance of the slab. Each narrow channel has viscous layers that absorb sound by the Konstantinov effect [2]. The energy reflected by the sheet increases for values close to the dense packing condition, allowing less sound to pass through and resulting in a smaller transmittance [5].

Moreover, the analytical results in Fig. 2 indicate that a reduction in the value of a_0 produces an increase in viscous losses. For a given frequency, absorption takes place mainly in the narrow channels between cylinders. For a fixed slab length, the number of layers forming the sheets and, consequently, the number of channels between cylinders grow in number as the lattice parameter a_0 is reduced, leading to an increase in absorption. Additionally, there is a displacement effect, possibly because of a stronger reflectance for larger a_0 values.

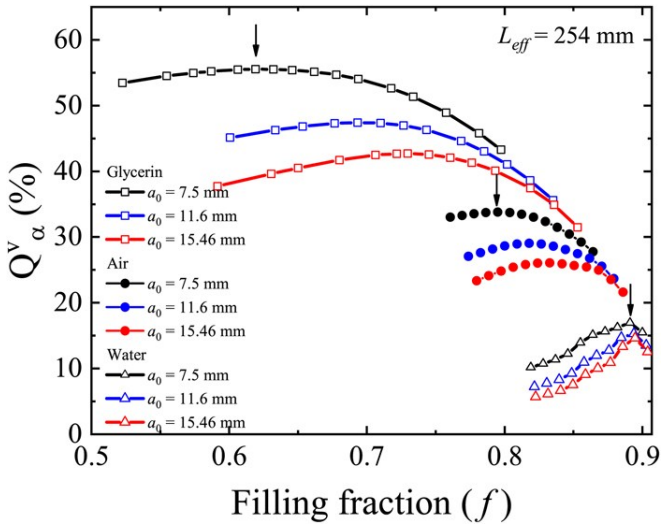

Figure 2: Variation of $\boldsymbol{Q_\alpha^v}$ as a function of the filling fraction of a homogenized slab for a fixed effective length $\boldsymbol{L_{eff}}$ and three different background media. The frequency range $\boldsymbol{\Delta\omega}$ is different as shown in Table 1. Absorption maxima are marked with arrows.

Another important aspect to analyze in the results shown in Fig. 2 is the dependence of Q_α^v on the background viscous medium. An interesting detail is the smaller absorption of water as compared with air. Water is more viscous than air, but its viscous layers are thinner than those in air (see Table 1). This is a result of the density of water being three orders of magnitude greater than that of air.

The existence of Fabry-Perot resonances caused by the finite thickness of the slab is the main mechanism that leads to viscous absorption. Therefore, we must be careful in selecting low frequency intervals such that the integral in Equation (5) contains several Fabry–Perot peaks.

The results reported here allow us to conclude that there is an optimal filling fraction f_{opt} rendering a maximum of absorption, represented by Q_α^v. In addition, for a given viscous background medium and for a fixed integration interval, a decrease of the lattice parameter a_0 leads to an increased overall Q_α^v.

Results for finite PnC clusters

Fig. 3 presents results of Q_α^v as a function of the filling fraction f for homogenized clusters of cylinders with circular external shape and a fixed effective radius R_{eff}= 0.748 m. The limits of integration for Equation (5) are $\omega_b = 2\pi \times$ 580 Hz and $\omega_t = 2\pi \times$ 3400 Hz, giving $\Delta\omega = 2\pi \times$ 2820 Hz.

We notice again the same phenomenon observed in slabs: the A cluster containing the largest number of cylinders provides the maximum viscous absorption in broadband despite having the same dimensions as the others. Clusters B and C, with 161 and 85 cylinders, respectively, provide

lower broadband absorption. The number of narrow channels for different lattice constants is, as in slabs, the plausible explanation of the observed behavior. This conclusion is supported by the maximum of Q_α^v exhibited by the clusters.

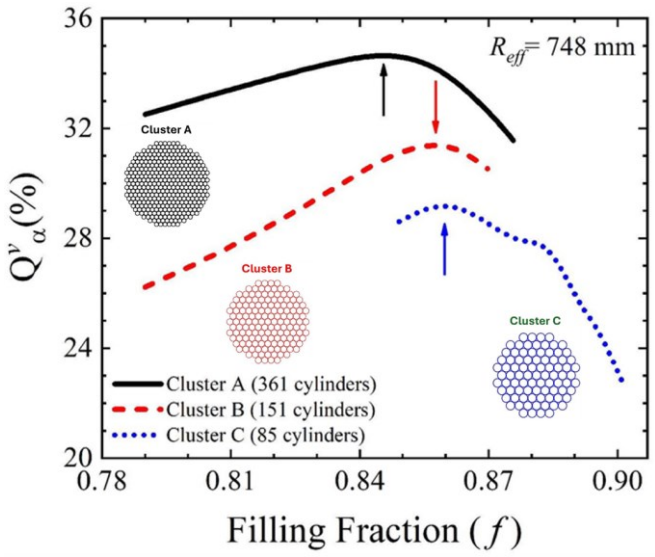

Figure 3: Variation of Q_α^v with f for three hard cylindrical clusters with the same effective radius and different number of internal cylinders. The frequency range used in Equation (5) is the same for all three structures. The arrows indicate the fraction with the highest absorption. The clusters are depicted alongside the curves.

Experimental validation

The results for a homogenized setup have been compared with simulations containing the cylinder lattices and measurements in a transmission tube, as shown in Fig. 4 [19]. The measured sample was 3D printed and has a cylindrical shape that fits in the transmission tube. The hexagonal lattice has a_0 = 11.1 mm and f = 0.8496. The homogenization in this case is valid for frequencies below 5000 Hz.

The lower section of Fig. 4 contains (a) the comparison of analytical, homogenized results with 2D FEM simulations, all in 2D and semi-infinite. In (b) the measurements are compared with an ad hoc simulation in 3D that represents the setup as it was measured. There are differences between the 2D and 3D results: the lattice contains now finite cylinders of different lengths, which is different from the 2D semi-infinite 2D version. The measurement system presents uncertainties as well and is sensitive to mounting conditions and dimensional tolerances. However, there is good agreement with measurements up to 5 kHz, the homogenization limit. The homogenization method is considered validated.

Conclusions

A semi-analytical model that allows the calculation of viscous absorbance in semi-infinite slabs of PnC, as well as in clusters of rigid cylinders with an external circular shape is presented. The structures are interesting because their absorption can be precisely controlled by varying its geometrical parameters. This is not the case with regular absorbing materials, subject to large uncertainties and only amenable to empirical and statistical descriptions. Simulations and experiments support the results presented here.

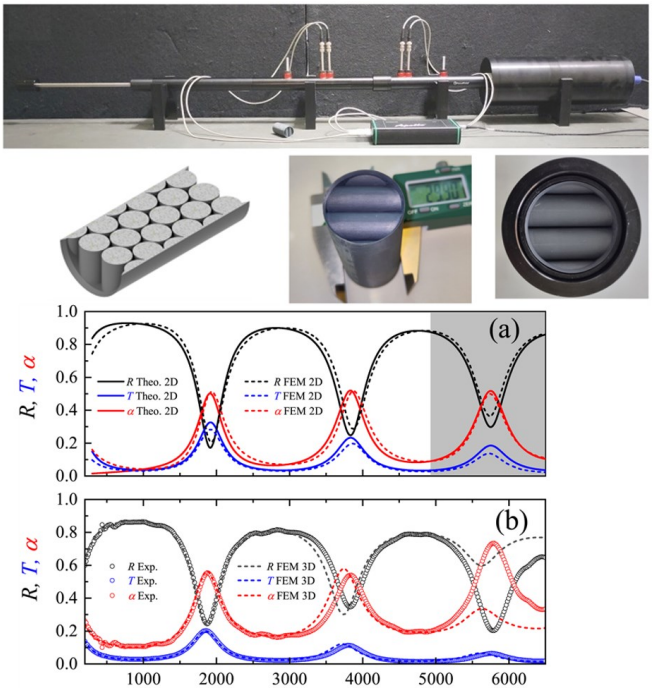

Figure 4: Above: Photographs and depictions of the PnC sample measured in the transmission tube of 30 mm diameter (AED AcoustiTube®). Below: (a) comparison of analytical homogenized calculations and FEM simulations in 2D, (b) Comparison of experimental and FEM results for a 3D sample with cylindrical shape. All results except those measured include viscous loses only.

The first relevant conclusion from the results is that there is an optimal value of the filling fraction, for each lattice, that achieves maximum absorption. This conclusion is demonstrated and discussed.

Secondly, it is shown that the amount of broadband dissipation is related to the density of narrow channels or necks within the PnC of finite or semi-infinite clusters. For cases with the same external dimension, greater dissipation is achieved for larger numbers of cylinders inside.

These results and conclusions are believed to be relevant for future research on the design of highly absorbent materials made of fibers.

Acknowledgements

Martin Ibarias thanks Jesús Arriaga for providing some computational resources for numerical calculations.

References

[1] G. Kirchhoff, (1868). Ann. d Phys. 134, 177.

[2] Konstantinov B.P., (1939). Zh. Eksp. Teor. Phys. 9, 226.

[3] Duclos, A., Lafarge, D., & Pagneux, V. (2009). Transmission of acoustic waves through 2D phononic crystal: Visco-thermal and multiple scattering effects. Epj Applied Physics, 45(1), 11302–p5. https://doi.org/10.1051/epjap:2008203

[4] Guild, M. D., Garcia-Chocano, V. M., Kan, W., & Sánchez-Dehesa, J. (2014). Enhanced inertia from lossy effective fluids using multi-scale sonic crystals. Aip Advances, 4(12), 124302. https://doi.org/10.1063/1.4901880

[5] Molerón, M., Serra-Garcia, M., & Daraio, C. (2016). Visco-thermal effects in acoustic metamaterials: From total transmission to total reflection and high absorption. New Journal of Physics, 18(3), 033003. https://doi.org/10.1088/1367-2630/18/3/033003

[6] Cutanda Henriquez, V., García-Chocano, V. M., & Sánchez-Dehesa, J. (2017). Viscothermal Losses in Double-Negative Acoustic Metamaterials. Physical Review Applied, 8(1), 014029. https://doi.org/10.1103/PhysRevApplied.8.014029

[7] Ibarias, M., Zubov, Y., Arriaga, J., & Krokhin, A. A. (2020). Phononic crystal as a homogeneous viscous metamaterial. Physical Review Research, 2(2), 022053. https://doi.org/10.1103/PhysRevResearch.2.022053

[8] Ibarias, M., Doporto, J., Krokhin, A. A., & Arriaga, J. (2022). Tuning the decay of sound in a viscous metamaterial. Philosophical Transactions of the Royal Society A: Mathematical, Physical and Engineering Sciences, 380(2237), 20220007. https://doi.org/10.1098/rsta.2022.0007

[9] Andersen, P. R., Cutanda Henriquez, V., & Aage, N. (2022). On the validity of numerical models for viscothermal losses in structural optimization for micro-acoustics. Journal of Sound and Vibration, 547, 117455. https://doi.org/10.1016/j.jsv.2022.117455

[10] Zhu, X. F., Lau, S. K., Lu, Z., & Jeon, W. (2019). Broadband low-frequency sound absorption by periodic metamaterial resonators embedded in a porous layer. Journal of Sound and Vibration, 461, 114922. https://doi.org/10.1016/j.jsv.2019.114922

[11] Zhang, X. H., & Qu, Z. G. (2022). Viscous and thermal dissipation during the sound propagation in the continuously graded phononic crystals. Applied Acoustics, 189, 108606. https://doi.org/10.1016/j.apacoust.2021.108606

[12] Cutanda Henriquez, V., & Sánchez-Dehesa, J. (2021). Visco-thermal effects in a two-dimensional acoustic black hole: A boundary element approach. Physical Review Applied, 15(6), 064057. https://doi.org/10.1103/PhysRevApplied.15.064057

[13] Xiong, L., Nennig, B., Aurégan, Y., & Bi, W. (2017). Sound attenuation optimization using metaporous materials tuned on exceptional points. Journal of the Acoustical Society of America, 142(4), 2288–2297. https://doi.org/10.1121/1.5007851

[14] Duan, H., Shen, X., Yang, F., Bai, P., Lou, X., & Li, Z. (2019). Parameter Optimization for Composite Structures of Microperforated Panel and Porous Metal for Optimal Sound Absorption Performance. Applied Sciences (Switzerland), 9(22), 4798. https://doi.org/10.3390/app9224798

[15] Garza Agudelo, D. M., Cutanda Henriquez, V., Jeong, C.-H., Andersen, P. R., Ibarias, M., Sánchez-Dehesa, J., & Lucklum, F. (2024). Metasurfaces for sound absorption over a broad range of wave incidence angles. Applied Acoustics, 220, 109965. https://doi.org/10.1016/j.apacoust.2024.109965

[16] Romero-García, V., & Hladky-Hennion, A. C. (2019). Ch. 1: Visco-thermal Effects in Acoustic Metamaterials Based on Local Resonances. In Fundamentals and Applications of Acoustic Metamaterials: From Seismic To Radio Frequency (pp. 1–300). Wiley. https://doi.org/10.1002/9781119649182

[17] Krokhin, A. A., Arriaga, J., & Gumen, L. N. (2003). Speed of sound in periodic elastic composites. Physical Review Letters, 91(26), 264302/1–4. https://doi.org/10.1103/PhysRevLett.91.264302

[18] Torrent, D., Håkansson, A., Cervera, F., & Sánchez-Dehesa, J. (2006). Homogenization of two-dimensional clusters of rigid rods in air. Physical Review Letters, 96(20), 204302. https://doi.org/10.1103/PhysRevLett.96.204302

[19] Ibarias, M., Cutanda Henríquez, V., Lucklum, F., & Sánchez-Dehesa, J. (2024). Broadband acoustic absorption at low frequencies by slabs and clusters made of hard cylindrical rods. Journal of Applied Physics, 136(4), 043104. https://doi.org/10.1063/5.0208386

[20] Ibarias, M. A., Henriquez, V. C., & Sánchez-Dehesa, J. (2024). Estudio de la absorción del sonido por pérdidas viscosas de arreglos de cilindros rígidos en un rango amplio de frecuencias. Proceedings of XLV Spanish Congress of Acoustics. http://www.spacustica.pt/acustica2024/index.html

[21] Cops, M. J., McDaniel, J. G., Magliula, E. A., Bamford, D. J., & Berggren, M. (2020). Estimation of acoustic absorption in porous materials based on visco-thermal boundary layers modeled as boundary conditions. Journal of the Acoustical Society of America, 148(3), 1624–1635. https://doi.org/10.1121/10.0001959

[22] Sanchis, L., Håkansson, A., Cervera, F., & Sánchez-Dehesa, J. (2003). Acoustic interferometers based on two-dimensional arrays of rigid cylinders in air. Physical Review B - Condensed Matter and Materials Physics, 67(3), 35422–35421-11. https://doi.org/10.1103/PhysRevB.67.035422

[23] Cutanda-Henríquez, V., & Juhl, P. M. (2013). An axisymmetric boundary element formulation of sound wave propagation in fluids including viscous and thermal losses. Journal of the Acoustical Society of America, 134(5), 3409–3418. https://doi.org/10.1121/1.4823840

[24] Cutanda Henriquez, V., Andersen, P. R., Jensen, J. S., Møller Juhl, P., & Sánchez-Dehesa, J. (2016). A Numerical Model of an Acoustic Metamaterial Using the Boundary Element Method Including Viscous and Thermal Losses. Journal of Computational Acoustics, 25(4), 1750006. https://doi.org/10.1142/S0218396X17500060